Published in final edited form as:
Mech Dev. 2012 September ; 129(9-12): 308–323. doi:10.1016/j.mod.2012.06.002.

Delayed fusion and altered gene expression contribute to semicircular canal defects in *Chd7* deficient mice

Elizabeth A. Hurd[1], **Joseph A. Micucci**[2], **Elyse N. Reamer**[1], and **Donna M. Martin**[1,3,*]

[1]Department of Pediatrics, The University of Michigan, Ann Arbor, Michigan, 48109

[2]Department of Biological Chemistry, The University of Michigan, Ann Arbor, Michigan, 48109

[3]Department of Human Genetics, The University of Michigan, Ann Arbor, Michigan, 48109

Summary

Proper morphogenesis of inner ear semicircular canals requires precise regulation of cellular proliferation, epithelial-to-mesenchymal transition, and fusion of epithelial plates. Epigenetic regulation of these processes is not well understood, but is likely to involve chromatin remodeling enzymes. CHD7 is a chromodomain-containing, ATP dependent helicase protein that is highly expressed in the developing ear and is required for semicircular canal development in both humans and mice. Here we report that mice with heterozygous loss of *Chd7* function exhibit delayed semicircular canal genesis, delayed *Netrin1* expression and disrupted expression of genes that are critical for semicircular canal formation (*Bmp2, Bmp4, Msx1 and Fgf10*). Complete loss of *Chd7* results in aplasia of the semicircular canals and sensory vestibular organs, with reduced or absent expression of *Otx1*, *Hmx3*, *Jagged1*, *Lmo4*, *Msx1* and *Sox2*. Our results suggest that *Chd7* may have critical selector gene functions during inner ear morphogenesis. Detailed analysis of the epigenetic modifications underlying these gene expression changes should provide insights into semicircular canal development and help in the design of therapies for individuals with inner ear malformations.

Keywords

CHD7; semicircular canal; cristae; chromatin remodeling; gene regulation; inner ear morphogenesis

Introduction

The mammalian inner ear is divided into two functionally distinct areas: the vestibular system (semicircular canals and associated cristae, saccule and utricle) which detects angular movement, and the auditory system (cochlea) which detects sound. Both vestibular and auditory compartments derive from a placodal thickening of the epithelium adjacent to rhombomeres 5 and 6 which invaginates to form the otocyst. During the early stages of otic development (E9-11.0 in mouse), the spherical otocyst undergoes major transformations to

*Correspondence to: 1150 W. Medical Center Dr. 3520A MSRB I Ann Arbor, MI 48109-5652 donnamm@umich.edu TEL: (734) 647-4859 FAX: (734) 763-9512 .

form a complex organ essential for hearing and balance perception (Kelley, 2006). Correct inner ear morphogenesis is dependent on axial patterning of gene expression throughout otic development (Sanchez-Calderon et al., 2007). Mutations in genes expressed in the dorsal otocyst (e.g. *Otx1, Hmx3, Dlx5*) result in semicircular canal defects, whereas mutations in ventrally expressed genes (e.g. *Ngn1, NeuroD*) result in cochlear defects (reviewed in Chatterjee et al., 2010; Fekete, 1999; Fekete and Wu, 2002).

Chromodomain-helicase-DNA-binding-protein 7 (CHD7) is a nuclear localized protein that is expressed in both the dorsal and ventral otocyst at E10.5, but later becomes restricted to the sensory epithelia, cochlea and cochleovestibular ganglion (Bosman et al., 2005; Hurd et al., 2010). Haploinsufficiency for *CHD7* in humans causes CHARGE syndrome, a multiple anomaly condition affecting ear, eye, heart, and craniofacial development (Vissers et al., 2004). A highly penetrant feature of CHARGE syndrome is semicircular canal hypoplasia/dysplasia which contributes to impaired balance sensation and delayed motor development in patients (Morimoto et al., 2006; Wiener-Vacher et al., 1999). Gene-trap derived and conditional null mutations of *Chd7* in mice also result in lateral and posterior semicircular canal defects and cochlear abnormalities (Adams et al., 2007; Hurd et al., 2007; Hurd et al., 2010). The mechanisms underlying semicircular canal defects in *Chd7* mutant mice are not known, but may be due to aberrant cellular proliferation, survival, and/or differentiation.

CHD7 contains two chromodomains, an ATP-dependent helicase domain and is thought to play a role in repression or activation of downstream target genes. CHD7 participates in large, multi-protein chromatin remodeling complexes that have complex epigenetic functions in diverse cell types and tissues (Takada et al., 2007; Woodage et al., 1997). Here we sought to explore the cellular mechanisms by which *Chd7* deficiency leads to abnormal morphogenesis of the semicircular canals through analysis of germline and conditional *Chd7* mutant embryos. We examined expression of otic patterning genes and genes involved in semicircular canal genesis. Our results support the hypothesis that *Chd7* acts as a critical, early selector gene by regulating expression of genes involved in multiple developmental processes and signaling pathways that are critical for normal vestibular morphogenesis.

Materials and Methods

Mice

Chd7$^{Gt/+}$ and *Chd7*$^{flox/flox}$ mice were genotyped as previously described (Hurd et al., 2007; Hurd et al., 2010). *Chd7*$^{Gt/+}$ mice were maintained by mating with $B6D_2F_1/J$ (Jackson Laboratory #100006) mice to generation N5-N7. *Foxg1-Cre* mice were maintained on a Swiss Webster background (Charles River Laboratories #F44481) and mated with *Chd7*$^{Gt/+}$ mice to generate *Foxg1-Cre;Chd7*$^{Gt/+}$ mice. *Chd7*$^{flox/flox}$ mice were interbred to generation N4-N5. Timed pregnancies were established with the morning of plug identification designated as E0.5. Embryos were collected after cervical dislocation and hysterectomy, and washed briefly in PBS. Amniotic sacs were collected and DNA isolated for PCR genotyping as described (Hurd et al., 2007). All procedures were approved by The University of Michigan University Committee on the Use and Care of Animals (UCUCA).

Paint filling

Timed pregnancies were established and embryos collected at E11.5, E12.5 and E13.5 after cervical dislocation and hysterectomy. Embryos were washed in PBS, fixed in Bodian's fixative, cleared using methyl salicylate and filled using 3% Whiteout (Hurd et al., 2007). At E11.5 ears from intact embryos were filled. At later time points, heads were bisected and the brain removed prior to paint filling to allow access to the inner ear.

Histology and Embedding

For paraffin sections, embryos were fixed in 4% paraformaldehyde for 30 minutes (E10.5) to 1.5 hrs. (E12.5), then washed in PBS and dehydrated in ethanol. Subsequently, embryos were embedded in paraffin and sectioned at 7 μm. For frozen sections, embryos were fixed and washed as described above, then incubated in 30% sucrose, embedded in OCT (Tissue Tek,Torrance CA), frozen, and cryosectioned at 12 μm. For histological analyses, sections were stained with Hematoxylin and Eosin (Sigma, St. Louis, MO) and photographed by light microscopy on a Leica upright DMRB microscope and processed in Photoshop CS2 (Adobe, San Jose, CA).

In situ hybridization

In situ hybridization was performed on either paraffin or frozen embedded embryo sections using digoxigenin-labeled riboprobes as previously described (Martin et al., 2002) at annealing temperatures between 55-65°C. For each probe, multiple sections from at least four ears ($N = 4$) of each genotype were tested. RNA probes for *Lmx1a, Lmo4, Msx1* and *Dlx5* were kindly provided by Doris Wu. Other probes used were *Netrin1* (Lisa Goodrich); *Bmp2* and *Bmp4* (Brigid Hogan); *Gbx2* (Luis Puelles). Primers were designed to *Otx1* (fwd: ATTCCATCCTTTACAGTTTGA; rev: TGGCCATAGGACATAGGGTAGGAG), *Gata3* (fwd: CTCCTTTTTGCTCTCCTTTTCTAT; rev: GTAATGGGGTGGTGGGCTGAGGAT) and *Hmx3* (fwd: TTCATTGGAAGTTTTGACCTGGTA; rev: GAGGCGGCCAACCTGAGC) and amplified by PCR. PCR products were cloned into pGEMT-easy (Promega, Madison, WI) and digoxigenin-labeled. Sections were photographed by light microscopy on a Leica upright DMRB microscope and processed in Photoshop CS2 (Adobe).

β-galactosidase staining

Frozen sections were air-dried, fixed in glutaraldehyde and washed with X-gal wash buffer (sodium phosphate buffer pH 7.4 with 2 mM MgCl2 and 0.02% NP-40 (Sigma)). Sections were stained in X-gal wash buffer containing 0.02 mg/ml X-gal (Roche, Indianapolis, IN) 5 mM potassium ferrocyanide (Fisher, Pittsburgh, PA), 5 mM potassium ferricyanide (Fisher), and 0.33% *N*-*N*-dimethylformamide (Sigma) and post-fixed in 4% paraformaldehyde. After counterstaining with eosin, sections were mounted and photographed using an upright Leica DMRB microscope and processed in Photoshop CS2 (Adobe).

Immunofluorescence

For paraffin section immunofluorescence, slides were de-waxed in xylene, endogenous peroxidase activity blocked with 3% H_2O_2 for 20 minutes, and nuclear epitopes exposed by boiling in 0.01 M citrate for 3 minutes. All subsequent washes were performed in PBS with 0.5% Tween 20. Polyclonal rabbit anti-SOX2 (AB5603, 1:250, Millipore, Billerica, MA); goat anti-JAGGED1 (SC6011, 1:100, Santa Cruz, Santa Cruz, CA) and rabbit anti-PAX2 (1:2000, gift of Greg Dressler) were incubated overnight at 4°C. Either direct secondary detection (Alexa488 or Alexa555 antibodies, Invitrogen) or indirect secondary detection using biotinylated antibodies (Vector Laboratories, Burlingame, CA) and HRP-streptavidin Tyramide signal amplification (Invitrogen) was performed. For each antibody, multiple sections from at least four ears ($N = 4$) of each genotype were tested. Sections were photographed by single channel fluorescence microscopy on a Leica upright DMRB microscope and processed in Photoshop CS2 (Adobe).

Cell proliferation

Immunofluorescence was performed as described above using rat anti-bromodeoxyuridine (BrdU) (Serotec, Raleigh, NC, 1:200) and rabbit anti-phosphohistone H3 (Millipore,

Billerica, MA, 1:200) followed by secondary detection with Alexa-conjugated antibodies (Invitrogen, 1:200) and co-stained with DAPI (Invitrogen, 1:50). Cell counts were performed on serial sections from at least 6 ears from 3 embryos for each genotype at each time point. Student *t*-tests with Welch's correction were performed to determine statistical significance of H3 and BrdU positive cells in the epithelium of the developing lateral canal. Standard error of the mean (s.e.m) was calculated for each value.

RNA isolation and quantitative real-time PCR

The inner ears of E10.5 *Chd7*$^{+/+}$, *Chd7*$^{Gt/+}$ and *Chd7*$^{Gt/Gt}$ littermate mice were microdissected and RNA was isolated using the RNAqueous-Micro RNA Isolation Kit (Ambion, Austin, TX, USA). Isolated RNA was treated with DNase I prior to cDNA synthesis. cDNA was generated using the Superscript First-Strand cDNA Synthesis System for quantitative real-time PCR with random primers (Invitrogen, Carlsbad, CA, USA). Relative gene expression levels were assayed using TaqMan Gene Expression Master Mix and TaqMan probes (Applied Biosystems, Foster City, CA, USA) for *Gapdh*, *Bmp2*, *Bmp4*, *Otx1* and *Sox2*. Each sample was run in triplicate using an Applied Biosystems StepOne-Plus Real-Time qPCR System. The gene expression level of *Gapdh* was used as an internal positive control. The difference in threshold cycle (C_T) between the assayed gene and *Gapdh* for any given sample was defined as the change in threshold cycle (ΔC_T). The difference in ΔC_T between two samples was defined as $\Delta\Delta C_T$ which represents a relative difference in expression of the assayed gene. The fold change of the assayed gene relative to *Gapdh* was defined as $2^{-\Delta\Delta CT}$. Unpaired t-test was performed on the *Gapdh*-normalized ΔC_T values to determine statistical significance of the gene expression changes ($p<0.05$).

Results

Heterozygous Chd7 mutant mice have delayed semicircular canal fusion

Semicircular canals in the mouse form via fusion of opposing walls of the developing canal pouch (Martin and Swanson, 1993). We previously demonstrated that germline (*Chd7*$^{Gt/+}$) or conditional heterozygous (*Foxg1-Cre;Chd7*$^{+/flox}$) loss of *Chd7* function results in lateral and posterior semicircular canal defects (Adams et al., 2007; Hurd et al., 2007; Hurd et al., 2010). Homozygous null (*Chd7*$^{Gt/Gt}$) embryos do not survive past E10.5 (Hurd et al., 2007), but *Foxg1-Cre Chd7* conditional null (CKO) inner mice survive until birth and have severe hypoplasia of the semicircular canals that is visible by E14.5 (Hurd et al., 2010). To investigate the onset of semicircular canal defects in *Chd7* mutant embryos, inner ear morphology was examined at E11.5-E13.5 by paint filling (Fig. 1). The epithelium of anterior, posterior and lateral canal pouches was fused in control inner ears, resulting in three semicircular canals (Fig 1 A,E,I). However, in *Chd7* heterozygous (*Chd7*$^{Gt/flox}$) and *Chd7* conditional heterozygous (*Foxg1-Cre;Chd7*$^{+/flox}$) embryos, fusion of the posterior (Fig. 1 asterisk) and lateral (Fig. 1 double asterisk) canals was incomplete, resulting in abnormally formed posterior and lateral semicircular canals (Fig 1. J, K). At E11.5, elongation of the cochlear duct in CKO embryos was similar to control embryos (Fig. 1D vs. 1A); however, the vestibular pouches were severely hypoplastic (Fig. 1 D). Although the endolymphatic duct was preserved in CKO ears, no semicircular canals were present and the cochlea was shortened and twisted. As inner ear development progressed up to E14.5 (Fig. 1 (Hurd et al., 2010)), there was minimal expansion, but no further morphogenetic change in the vestibular area in *Chd7* heterozygous or CKO inner ears. Thus, defects in semicircular canal genesis in *Chd7* mutant mice occur as early as E11.5 during early inner ear development.

To investigate whether defects in canal plate fusion were responsible for the semicircular canal defects observed in *Chd7* mutants (Adams et al., 2007; Hurd et al., 2007; Hurd et al.,

2010), we analyzed Hematoxylin and Eosin (H&E) stained ear sections at E11.5-E12.5. At E11.5, there were no differences in the morphology of the lateral (Fig. 2D) or anterior/posterior (Supplemental Fig. 1D) pouches in *Chd7* conditional heterozygotes compared to controls (Fig. 2A and Supplemental Fig. 1). By E12.0 control embryos, the anterior/posterior and lateral canal epithelia were detached from the basement membrane (arrows in Fig. 2B and Supplemental Fig. 1B), consistent with ongoing morphological changes at the basement membrane/epithelial interface. Following detachment, the anterior/posterior and lateral epithelia fuse to form canals (Fig. 2C and Supplemental Fig. 1C). In contrast, *Chd7* conditional heterozygotes exhibited no detachment of the basement membrane at E12.0 in either the anterior/posterior (Supplemental Fig. 1E) or lateral (Fig. 2E) semicircular canal pouches. Instead, basement membrane detachment was observed at E12.5 in conditional heterozygous embryos (Fig. 2F), constituting a delay of approximately 0.5 days.

Chd7 conditional null (CKO) inner ears were extremely hypoplastic at E11.5 (Fig. 1, Fig.2G and Supplemental Fig. 1G); however, the endolymphatic duct appeared normal (Supplemental Fig. 1G-I). A small canal pouch was present at E11.5-E12.0 in the caudal region of the hypoplastic *Chd7* conditional null inner ear (Fig 2. G, H), similar to the small pouch observed by paint filling (Fig. 1D). These data provide evidence to support an earlier hypothesis that semicircular canal defects in *Chd7* deficient mice result from delays in fusion plate formation (Bosman et al., 2005; Kiernan et al., 2002).

Expression of genes involved in lateral otic patterning is reduced in Chd7 mutant otocysts

Otic patterning, defined by gene expression domains, is essential for correct development of vestibular and auditory systems (Alsina et al., 2009; Bok et al., 2007). *Chd7* is highly expressed in the otic epithelium, cochleovestibular ganglion and mesenchyme at E10.5 (Bosman et al., 2005; Hurd et al., 2010; Randall et al., 2009). To test whether reduced *Chd7* disrupts dorsal and medial otocyst patterning, we examined markers of dorsal and medial otocyst (*Lmx1a*, *Dlx5*, *Gbx2* and PAX2) in E10.5 *Chd7* heterozygous (*Chd7*$^{Gt/+}$ and *Foxg1-Cre:Chd7*$^{+/flox}$) and *Chd7* null (*Chd7*$^{Gt/Gt}$ and *Foxg1-Cre:Chd7*$^{Gt/flox}$) embryos. We observed normal expression of genes in dorsal (*Lmx1a, Dlx5*) and medial (*Gbx2,* PAX2) domains of *Chd7* heterozygous and *Chd7* conditional-null (CKO) otocysts (Fig. 3). Expression of *Lmx1a*, *Dlx5*, *Gbx2* and PAX2 protein were also preserved in *Chd7*$^{Gt/Gt}$ otocysts (Fig. 3. C, H, M and R), despite their severe hypoplasia.

The dorsolateral compartment of the developing otocyst gives rise to the semicircular canals (Fekete and Wu, 2002). Since *Chd7* heterozygous and CKO mutant mice have semicircular canal defects, we analyzed expression of genes within the lateral domain of developing *Chd7* mutant otocysts at E10.5 (Fig. 4). *Otx1*, *Hmx3, Lmo4* and *Gata3* expression were preserved in *Chd7* heterozygous (*Chd7*$^{Gt/+}$ and *Foxg1-Cre:Chd7*$^{+/flox}$) otocysts compared with *Chd7*$^{+/+}$. Expression of *Hmx3*, *Lmo4* and *Gata3* within the ventral domain of E10.5 otocysts was also preserved within CKO otocysts (Fig. 4 J, O, Y). However, expression of *Otx1* and dorsal *Gata3* were reduced in CKO embryos (Fig. 4 E, T). Although ventromedial expression of *Gata3* was present in *Chd7*$^{Gt/Gt}$ otocysts, dorsolateral expression of *Otx1*, *Hmx3*, *Lmo4* and *Gata3* were absent from *Chd7* null embryos. These data indicate that *Chd7* is required for dorsolateral patterning of the developing otocyst.

We also examined changes in gene expression during vestibular morphogenesis, but after axial otocyst patterning (E11.5), in *Chd7* mutant mice. There were no differences in expression of dorsomedial (*Lmx1a*, *Gbx2* and *Dlx5)* or dorsolateral (*Otx1, Dlx5* and *Hmx3)* genes between *Chd7*$^{+/flox}$ and *Chd7* heterozygous embryos at E11.5 (Fig. 5). Expression of *Lmx1a*, *Gbx2, Hmx3* and medial expression of *Dlx5* was also preserved in CKO embryos at E11.5 (Fig. 5 D, H, P, T). In contrast, lateral expression of *Dlx5* and *Otx1* was absent from CKO inner ears (Fig. 5 L, P). Interestingly, *Chd7* appears to have minimal influence on

genes expressed in the dorsomedial domain. These data suggest that loss of *Chd7* affects patterning of the lateral otocyst and regulates expression of *Otx1* within the otocyst.

Netrin1 expression is altered in Chd7 mutant mice

Defects in semicircular canal formation can be caused by disrupted morphogenetic gradients within the inner ear, which affect formation of the fusion plate and/or movement of cells that ultimately contribute to canal development (Martin and Swanson, 1993). To explore the underlying mechanisms resulting in delayed semicircular canal genesis in *Chd7* mutant mice, we first examined expression of *Netrin1,* an extracellular matrix molecule that is critical for formation of the canal fusion plate (Salminen et al., 2000). *Netrin1* null mice have severe semicircular canal abnormalities, including absent lateral and posterior canals, and smaller anterior canals (Salminen et al., 2000).

β-galactosidase reporter activity in $Chd7^{Gt/+}$ embryos demonstrated *Chd7* expression in the canal epithelium and mesenchyme at E11.5 (Fig. 6A) and E12.5 (Fig. 6B). At E11.5, *Netrin1* was expressed in a medial domain of the developing posterior semicircular canal and a lateral domain within the posterior/ lateral semicircular canals of wild type embryos (Fig. 6C), with a similar expression pattern at E12.5 (Fig. 6D). In E11.5 $Chd7^{Gt/+}$ and conditional *Chd7* heterozygotes, the medial expression domain of *Netrin1* was absent from the posterior semicircular canal epithelium (asterisks in Fig. 6C, D). *Netrin1* was expressed within the hypoplastic canal epithelium of *Chd7* conditional null embryos (Fig 6E, J), suggesting that lack of medial *Netrin1* expression in E11.5 mutants represents delayed expression rather than direct regulation by *Chd7*. Delayed *Netrin1* expression in the developing mutant fusion plate could prevent appropriate breakdown of the basement membrane at the correct time, thereby disrupting canal formation.

Prior studies in chick showed that treatment of embryos with Noggin (a Bmp antagonist) disrupts canal formation at multiple stages, including canal pouch outgrowth and formation (Chang et al., 1999; Chang et al., 2002). A *Bmp2*-positive canal genesis zone located adjacent to the developing crista is essential for proper morphogenesis of the semicircular canals (Chang et al., 2004). We observed absence of *Bmp2* expression within the canal epithelium of the developing E12.5 $Chd7^{Gt/+}$ inner ear (Fig. 7D), despite normal levels of *Bmp2* expression in the anterior and posterior canal primordia (Fig. 7C). Absence of *Bmp2* expression specifically in the lateral semicircular canal in *Chd7* mutants is intriguing and may partly explain why the lateral semicircular canal is more sensitive to reduced *Chd7* function.

Altered proliferation in the $Chd7^{Gt/+}$ lateral canal and surrounding mesenchyme

Proliferation within the periotic mesenchyme and otic epithelium are essential to promote proper semicircular canal genesis (Haddon and Lewis, 1991; Lang et al., 2000). *Chd7* is expressed in both the developing otic epithelium and periotic mesenchyme during semicircular canal development (Fig. 6 and (Bosman et al., 2005; Hurd et al., 2010)). Therefore, any alterations in proliferation in either the lateral canal epithelium or surrounding mesenchyme may contribute to lateral canal abnormalities observed in *Chd7* heterozygous mice. We examined cellular proliferation in the lateral canal epithelium and surrounding mesenchyme at E11.0-E12.0 using immunofluorescence with anti-BrdU and anti-phosphohistone-H3. Proliferating cells within the lateral canal epithelium were defined as those in the most dorsal and lateral regions of the otic epithelium (solid lines in Fig.8), and proliferating cells in the area between the most dorsal and lateral points were defined as mesenchymal cells (area within dotted lines in Fig. 8). We observed a significant decrease (33%; p=0.035) in the number of H3-positive cells in the epithelium at E11.0 in $Chd7^{Gt/+}$ mice compared to wild type embryos (Fig. 8). In the mesenchyme, we also observed

significant reductions in the numbers of H3-positive (57%; p= 0.0005) and BrdU-positive (59%; p< 0.0001) cells at E11.0. At E11.5, there were no differences in numbers of BrdU-positive or H3-positive cells in the lateral epithelium or mesenchyme compared to wild type (Fig. 8). Likewise, there were no differences in proliferation in the lateral epithelium at E12.0 between *Chd7*$^{Gt/+}$ and wild type mice (Fig.8M and N). In contrast, there were significant increases in H3-positive (59%; p=0.013) and BrdU-positive (54%; p=0.003) cells in the *Chd7 Gt/+* mesenchyme relative to wild type at E12.0. Excess proliferation during this critical time for semicircular canal development in *Chd7*$^{Gt/+}$ embryos may result in increased cellular mass, preventing the epithelium from detaching normally from the basement membrane for subsequent fusion.

Chd7 is required for proper gene expression in the developing vestibular sensory epithelium

Correct specification of the prosensory otic epithelium is essential for the development of sensory hair cells and proper semicircular canal development (Fekete and Campero, 2007; Kelley, 2006). *Jag1*, *Sox2* and *Bmp4* are expressed in prosensory domains of the inner ear during otic development, and mutation of these genes in mice results in semicircular canal defects (Kiernan et al., 2001; Kiernan et al., 2005; Morsli et al., 1998; Tsai et al., 2001; Winnier et al., 1995). We found no differences in the presence of JAG1, a Notch ligand, or SOX2 in E10.5 otocysts of heterozygous *Chd7* mutants (Fig. 9B,D and G,I) or *Chd7* conditional knockouts (Fig. 9E and J) compared to control embryos (Fig. 9A and F). In contrast, SOX2 immunoreactivity was absent from *Chd7*$^{Gt/Gt}$ otocysts (Fig. 9H). *Bmp4* was expressed in the anterior crista primordium in *Chd7*$^{Gt/+}$ and *Chd7* conditional mutants at E10.5 (Fig. 9 L,N). In the majority of *Chd7*$^{Gt/+}$ ears, the *Bmp4*-positive posterior streak expression was also present (Fig. 9 Q; N=4/6). *Bmp4* expression was absent from E10.5 otocysts of both *Chd7*$^{Gt/Gt}$ (Fig. 9 M,R) and *Chd7* conditional null (Fig. 9 O,T) embryos. Thus, *Chd7* regulates expression of *Bmp4* and *Sox2* within the developing vestibular prosensory domain but does not significantly affect JAG1.

Formation of the cristae is dependent on normal expression of *Bmp4* (Chang et al., 2008). Therefore we examined expression of *Bmp4,* JAG1 and SOX2 on adjacent sections at E11.5 and E12.5, when the lateral crista forms a distinct prosensory domain and semicircular canal formation has begun (Fig. 10). Expression of *Bmp4* and JAG1 and SOX2 protein were preserved in the anterior cristae of all *Chd7* heterozygous embryos at E11.5 and E12.5 (data not shown). *Bmp4* mRNA and JAG1 and SOX2 protein were present in the lateral cristae of *Chd7* conditional heterozygotes at E11.5 (Fig. 10 G-I) and E12.5 (Supplemental Fig. 2). *Bmp4* expression was variably absent from the lateral cristae (N=2/4) of *Chd7*$^{Gt/flox}$ embryos despite the presence of JAG1 and SOX2 in the same prosensory region at E11.5 (Fig. 10 M-O) and E12.5 (Supplemental Fig. 2). In addition, *Fgf10* expression was reduced in the lateral (n=6/6) and posterior cristae (n=6/6) of *Chd7*$^{Gt/+}$ embryos at E12.5 (Supplemental Fig. 3B). No *Bmp4*, JAG1 or SOX2 were detected in the dorsal compartment of CKO inner ears at E11.5 (Fig. 10 S-U) and E12.5 (Supplemental Figure 2). These results suggest that genes expressed within the presumptive crista are particularly sensitive to *Chd7* dosage.

Bmp4 functions in the crista to organize sensory and non-sensory domains by regulating expression of *Msx1* and *Lmo4* in the sensory epithelium and *Gata3* and *Lmo4* in the non-sensory epithelium (Chang et al., 2008). Adult *Chd7*$^{Gt/+}$ mice have defects in the posterior cristae and variable absence of lateral ampullae (Adams et al., 2007); therefore, we analyzed expression of *Gata3*, *Lmo4* and *Msx1* in *Chd7* mutant embryos at E11.5. We observed normal expression of *Gata3* and *Lmo4* in *Chd7* heterozygous embryos (Fig. 10 J, K and P, Q), and absent *Gata3* and *Lmo4* expression in *Chd7* CKO inner ears (Fig. 10 V,W). Medial expression of *Msx1* was preserved in all *Chd7* mutant embryos, consistent with normal

development of the endolymphatic duct (Fig. 10F, L, R, X). In contrast, lateral expression of *Msx1* was preserved in conditional heterozygotes but was absent in $Chd7^{Gt/flox}$ and *Chd7* CKO embryos. Decreased expression of *Bmp4, Msx1* and *Fgf10* in $Chd7^{Gt/flox}$ ears likely contributes to the hypoplastic lateral cristae and posterior crista malformations observed in adult $Chd7^{Gt/+}$ mice (Adams et al., 2007).

We utilized quantitative real-time PCR (qRT-PCR) to more precisely define gene expression changes observed in the developing otocyst with decreased *Chd7* dosage. Expression of *Bmp2*, *Bmp4*, *Sox2*, *Fgf10* and *Otx1* were measured in microdissected E10.5 otocysts from wild type, $Chd7^{Gt/+}$ and $Chd7^{Gt/Gt}$ embryos (Fig. 11). *Bmp2* was reduced by 40% in $Chd7^{Gt/+}$ and 85% in $Chd7^{Gt/Gt}$ otocysts relative to wild type. *Bmp4* was reduced by 4% in $Chd7^{Gt/+}$ and 45% in $Chd7^{Gt/Gt}$ otocysts relative to wild type. *Sox2* was reduced by 12% in $Chd7^{Gt/+}$ and 83% in $Chd7^{Gt/Gt}$ otocysts. *Otx1* was reduced by 28% in $Chd7^{Gt/+}$ and 99% in $Chd7^{Gt/Gt}$ otocysts and *Fgf10* was reduced by 36% in $Chd7^{Gt/+}$ and 80% in $Chd7^{Gt/Gt}$ otocysts. Interestingly, *Bmp4* and SOX2 appeared to be absent by *in situ* hybridization and immunofluorescence, respectively, in $Chd7^{Gt/Gt}$ otocysts, but were detectable by qRT-PCR. This may be due to higher sensitivity for detecting low levels of gene expression. Together, our data indicate that *Chd7* is important for regulating expression of genes known to be critical for proper development of the semicircular canals and their associated cristae.

Discussion

Here we present a detailed analysis of developing inner ears with varying *Chd7* dosage (wild type, heterozygous and homozygous null, conditional heterozygous null and conditional null). We observed changes in expression of several genes known to be critical for semicircular canal formation (Table 1). Changes in expression of key genes in the otocyst and presumptive crista primordium are summarized in Figure 12.

Genes expressed in the presumptive crista and canal primordium are particularly sensitive to loss of Chd7

We found that complete loss of *Chd7* in the developing otocyst disrupts gene expression in a regionally restricted manner. Loss of *Chd7* has no effect on genes expressed in the dorsomedial otocyst (*Dlx5, Gbx2, Lmx1a*). In contrast, genes expressed in the presumptive crista (*Bmp4*, *Fgf10*, *Gata3, Jag1, Lmo4, Msx1,* and *Sox2*) are down-regulated in CKO mutants (Fig. 12A). Mutations in these crista-expressed genes disrupt crista formation and development of the semicircular canals (Chang et al., 2008; Deng et al., 2010; Kiernan et al., 2001; Kiernan et al., 2005; Lillevali et al., 2004; Pauley et al., 2003). Absence of *Bmp4, Fgf10*, *Jag1,* and *Sox2* in the *Chd7* CKO mutant helps explain the hypoplasia of the vestibular apparatus, as loss of any one of these genes is sufficient to disrupt canal formation. Conditional loss of *Bmp4* using *Foxg1-Cre* mice results in highly penetrant defects of semicircular canals and their associated cristae, with preservation of the endolymphatic duct (Chang et al., 2008). Since *Bmp4* also acts upstream of *Gata3*, *Lmo4*, and *Msx1*, disruption of these genes in *Chd7* mutants may be secondary to reduced *Bmp4* (Fig. 12).

Homozygous loss of *Fgf10* (Pauley et al., 2003), *Sox2* (Kiernan et al., 2005) or conditional loss of *Jag1* (Kiernan et al., 2001) results in milder semicircular canal defects than those observed in *Chd7* CKO mice, even though expression of *Fgf10*, *Sox2* and *Jag1* is insensitive to changes in *Bmp* signaling (REF Chang 2008). Thus, combined loss of *Bmp4, Fgf10*, *Sox2* and *Jag1* likely explains the severity of canal defects observed in *Chd7* mutants. Interestingly, CHD7 and SOX2 interact in neural stem cells to regulate expression of *Jag1* (Engelen et al., 2011). Since *CHD7* function is tissue- and developmental stage specific, it will be important to confirm this SOX2-CHD7 interaction in the inner ear.

We also observed reduced expression of some canal-associated genes (*Netrin1* and *Bmp2*) in heterozygous *Chd7* mutant ears. *Netrin1* expression is delayed but not absent in the *Chd7* mutant canal primordium. *Netrin1* mutant mice have disrupted semicircular canals and defects in fusion of the canal primordia (Salminen et al., 2000). In *Chd7* mutant mice, the canal plates undergo delayed fusion, concomitant with *Netrin1* expression, suggesting that disrupted onset of *Netrin1* expression does not cause the fusion delay. During canal development, *Bmp2* expression in the canal primordium is regulated by *Bmp4* and by *Fgf10* (Chang et al., 2004; Chang et al., 2008). Reduced *Bmp4* or *Fgf10* in *Chd7* mutants could therefore explain both the reduction in *Bmp2* expression and the semicircular canal defects. The similarities in phenotypes, expression profiles, and effects on downstream targets in *Fgf10, Bmp4* and *Chd7* mutant mice strongly suggest that they share common developmental signaling pathways.

In the lateral *Chd7* mutant otocyst, *Otx1* expression is reduced but expression of *Hmx3* is preserved. *Otx1* is essential in mice for development of the lateral semicircular canal (Acampora et al., 1996; Morsli et al., 1999). *Otx1* is expressed only in the lateral (not in anterior or posterior) canal, and *Otx1* mutant mice have only lateral canal defects (Morsli et al., 1999). Thus, absence of *Otx1* in the *Chd7* CKO otocyst could contribute to the severe lateral canal defects, but is unlikely to explain the loss of anterior and posterior canals. Interestingly, *Otx1* expression is unchanged in *Chd7* heterozygous mice despite the highly penetrant lateral canal defects (Adams et al., 2007; Hurd et al., 2007; Hurd et al., 2010). Since *Otx2* expression is also reduced in *Chd7* mutant otocysts in a dosage dependent manner (Hurd et al., 2010), *Otx* gene family members may be direct downstream targets of *Chd7* in the inner ear. Like *Otx1*, *Hmx3* is essential for development of the lateral semicircular canal and associated crista (Wang et al., 1998). However, in *Chd7* mutants, *Hmx3* expression is conserved, as it is in *Bmp4* conditional null otocysts (Chang et al., 2008). The differential effects of *Chd7* deficiency on *Otx1* and *Hmx3* expression in the lateral canal underscore the complex and pleiotropic roles for *Chd7* in gene regulation and inner ear development.

Dosage, timing, and tissue specificity of Chd7 in ear development

Inner ear morphogenesis is exquisitely sensitive to gene dosage and spatiotemporal changes in gene expression (Bok et al., 2007). We show that reduced *Chd7* in the inner ear leads to *Chd7* dosage-dependent changes in gene expression and progressively more severe inner ear defects. For example, *Hmx3, Lmo4,* and *Sox2* expression are preserved in *Chd7* conditional null otocysts, but are absent in $Chd7^{Gt/Gt}$. *Foxg1-Cre* deletes *Chd7* in the otocyst with minimal or no *Cre* activity in surrounding mesenchyme (whereas *Chd7* is expressed in both the epithelium and mesenchyme); thus, changes in gene expression and vestibular defects in *Chd7* conditional mutants may reflect epithelial-specific roles for *Chd7*. The severity of semicircular canal defects in *Chd7* CKO mice using *Foxg1-Cre* indicates that semicircular canal defects associated with *Chd7* deficiency are of epithelial origin. The influence of *Chd7* in the periotic mesenchyme and hindbrain on semicircular canal formation remains to be determined (Adams et al., 2007; Hurd et al., 2007; Hurd et al., 2010). Future experiments to address this include examining inner ear development in *Chd7* conditional mice using mesenchymal-specific and hindbrain-specific *Cre* lines.

Differential changes in gene expression between conditional and germline mutants may also reflect the timing of *Cre*-mediated *Chd7* deletions. In *Foxg1-Cre* mice, *Cre* is active in the otocyst by E8.5, based on reporter analysis in developing embryos (Hebert and McConnell, 2000). Changes in the timing of gene expression may be especially disruptive for lateral canal formation, based on the complete penetrance of lateral canal defects in germline heterozygous *Chd7* mutant mice (Adams et al., 2007; Hurd et al., 2007; Hurd et al., 2010).

Chd7 may function as a selector gene for semicircular canal formation

We identified several genes with unchanged expression in *Chd7* mutant embryos, indicating that specific genetic pathways are preserved with *Chd7* deficiency. CHD7 is predicted to bind to thousands of sites in the mammalian genome (Schnetz et al., 2009), and a major challenge is to identify those genes and gene pathways that mediate effects of CHD7 in cells and tissues. The specificity of *Chd7* function is also of general interest in understanding how chromatin structure contributes to development. Genes encoding transcription factors that are essential for the formation of specific organs, tissues and cell types have been termed "selector genes" (Crickmore and Mann, 2008; Mann and Carroll, 2002). Mutations in selector genes result in absence of specific organs or tissues due to changes in expression of networks of downstream regulated genes, and these gene expression changes are often non-linear and very complex. To date, only one inner ear specific gene, *Tbx1*, has been considered a selector gene (Raft et al., 2004). Interestingly, *Tbx1* is up-regulated by loss of *Chd7* (Hurd et al., 2010) and *Tbx1* conditional null mice, generated with *Foxg1-Cre* (Arnold et al., 2006), display a semicircular canal phenotype that resembles *Chd7* conditional mutant mice. Since *Chd7* mutant mice have severely hypoplastic vestibular structures and decreased expression of genes involved in multiple signaling pathways in the inner ear, we propose that *Chd7* may also act as a selector gene for semicircular canal genesis. Further studies will help determine whether *Chd7* regulates expression of these genes directly or indirectly as part of distinct signaling cascades.

Supplementary Material

Refer to Web version on PubMed Central for supplementary material.

Acknowledgments

We thank Greg Dressler, Lisa Goodrich, Brigid Hogan, Luis Puelles and Doris Wu who kindly provided *in situ* probes and antibodies for this project. This work was supported by NIH T32 grant DC00011 (JAM) and NIH grant DC009410 (DMM).

References

Acampora D, Mazan S, Avantaggiato V, Barone P, Tuorto F, Lallemand Y, Brulet P, Simeone A. Epilepsy and brain abnormalities in mice lacking the Otx1 gene. Nature Genetics. 1996; 14:218–22. [PubMed: 8841200]

Adams ME, Hurd EA, Beyer LA, Swiderski DL, Raphael Y, Martin DM. Defects in vestibular sensory epithelia and innervation in mice with loss of Chd7 function: implications for human CHARGE syndrome. J Comp Neurol. 2007; 504:519–32. [PubMed: 17701983]

Alsina B, Giraldez F, Pujades C. Patterning and cell fate in ear development. Int J Dev Biol. 2009

Arnold JS, Braunstein EM, Ohyama T, Groves AK, Adams JC, Brown MC, Morrow BE. Tissue-specific roles of Tbx1 in the development of the outer, middle and inner ear, defective in 22q11DS patients. Hum Mol Genet. 2006; 15:1629–39. [PubMed: 16600992]

Bok J, Chang W, Wu DK. Patterning and morphogenesis of the vertebrate inner ear. Int J Dev Biol. 2007; 51:521–33. [PubMed: 17891714]

Bosman EA, Penn AC, Ambrose JC, Kettleborough R, Stemple DL, Steel KP. Multiple mutations in mouse Chd7 provide models for CHARGE syndrome. Hum Mol Genet. 2005; 14:3463–76. [PubMed: 16207732]

Chang W, Brigande JV, Fekete DM, Wu DK. The development of semicircular canals in the inner ear: role of FGFs in sensory cristae. Development. 2004; 131:4201–11. [PubMed: 15280215]

Chang W, Lin Z, Kulessa H, Hebert J, Hogan BL, Wu DK. Bmp4 is essential for the formation of the vestibular apparatus that detects angular head movements. PLoS Genet. 2008; 4:e1000050. [PubMed: 18404215]

Chang W, Nunes FD, De Jesus-Escobar JM, Harland R, Wu DK. Ectopic noggin blocks sensory and nonsensory organ morphogenesis in the chicken inner ear. Dev Biol. 1999; 216:369–81. [PubMed: 10588886]

Chang W, ten Dijke P, Wu DK. BMP pathways are involved in otic capsule formation and epithelial-mesenchymal signaling in the developing chicken inner ear. Dev Biol. 2002; 251:380–94. [PubMed: 12435365]

Chatterjee S, Kraus P, Lufkin T. A symphony of inner ear developmental control genes. BMC Genet. 2010; 11:68. [PubMed: 20637105]

Crickmore MA, Mann RS. The control of size in animals: insights from selector genes. Bioessays. 2008; 30:843–53. [PubMed: 18693263]

Deng M, Pan L, Xie XL, Gan L. Requirement for Lmo4 in the vestibular morphogenesis of mouse inner ear. Developmental Biology. 2010; 338:38–49. [PubMed: 19913004]

Engelen E, Akinci U, Bryne JC, Hou J, Gontan C, Moen M, Szumska D, Kockx C, van Ijcken W, Dekkers DH, Demmers J, Rijkers EJ, Bhattacharya S, Philipsen S, Pevny LH, Grosveld FG, Rottier RJ, Lenhard B, Poot RA. Sox2 cooperates with Chd7 to regulate genes that are mutated in human syndromes. Nat Genet. 2011; 43:607–11. [PubMed: 21532573]

Fekete DM. Development of the vertebrate ear: insights from knockouts and mutants. Trends Neurosci. 1999; 22:263–9. [PubMed: 10354604]

Fekete DM, Campero AM. Axon guidance in the inner ear. Int J Dev Biol. 2007; 51:549–56. [PubMed: 17891716]

Fekete DM, Wu DK. Revisiting cell fate specification in the inner ear. Curr Opin Neurobiol. 2002; 12:35–42. [PubMed: 11861162]

Haddon CM, Lewis JH. Hyaluronan as a propellant for epithelial movement: the development of semicircular canals in the inner ear of Xenopus. Development. 1991; 112:541–50. [PubMed: 1794322]

Hebert JM, McConnell SK. Targeting of cre to the Foxg1 (BF-1) locus mediates loxP recombination in the telencephalon and other developing head structures. Dev Biol. 2000; 222:296–306. [PubMed: 10837119]

Hurd EA, Capers PL, Blauwkamp MN, Adams ME, Raphael Y, Poucher HK, Martin DM. Loss of Chd7 function in gene-trapped reporter mice is embryonic lethal and associated with severe defects in multiple developing tissues. Mamm Genome. 2007; 18:94–104. [PubMed: 17334657]

Hurd EA, Poucher HK, Cheng K, Raphael Y, Martin DM. The ATP-dependent chromatin remodeling enzyme CHD7 regulates pro-neural gene expression and neurogenesis in the inner ear. Development. 2010; 137:3139–50. [PubMed: 20736290]

Kelley MW. Regulation of cell fate in the sensory epithelia of the inner ear. Nat Rev Neurosci. 2006; 7:837–49. [PubMed: 17053809]

Kiernan AE, Ahituv N, Fuchs H, Balling R, Avraham KB, Steel KP, Hrabe de Angelis M. The Notch ligand Jagged1 is required for inner ear sensory development. Proc Natl Acad Sci U S A. 2001; 98:3873–8. [PubMed: 11259677]

Kiernan AE, Erven A, Voegeling S, Peters J, Nolan P, Hunter J, Bacon Y, Steel KP, Brown SD, Guenet JL. ENU mutagenesis reveals a highly mutable locus on mouse Chromosome 4 that affects ear morphogenesis. Mamm Genome. 2002; 13:142–8. [PubMed: 11919684]

Kiernan AE, Pelling AL, Leung KK, Tang AS, Bell DM, Tease C, Lovell-Badge R, Steel KP, Cheah KS. Sox2 is required for sensory organ development in the mammalian inner ear. Nature. 2005; 434:1031–5. [PubMed: 15846349]

Lang H, Bever MM, Fekete DM. Cell proliferation and cell death in the developing chick inner ear: spatial and temporal patterns. J Comp Neurol. 2000; 417:205–20. [PubMed: 10660898]

Lillevali K, Matilainen T, Karis A, Salminen M. Partially overlapping expression of Gata2 and Gata3 during inner ear development. Developmental Dynamics. 2004; 231:775–781. [PubMed: 15499560]

Mann RS, Carroll SB. Molecular mechanisms of selector gene function and evolution. Curr Opin Genet Dev. 2002; 12:592–600. [PubMed: 12200165]

Martin DM, Skidmore JM, Fox SE, Gage PJ, Camper SA. Pitx2 distinguishes subtypes of terminally differentiated neurons in the developing mouse neuroepithelium. Dev Biol. 2002; 252:84–99. [PubMed: 12453462]

Martin P, Swanson GJ. Descriptive and experimental analysis of the epithelial remodellings that control semicircular canal formation in the developing mouse inner ear. Dev Biol. 1993; 159:549–58. [PubMed: 8405678]

Morimoto AK, Wiggins RH 3rd, Hudgins PA, Hedlund GL, Hamilton B, Mukherji SK, Telian SA, Harnsberger HR. Absent semicircular canals in CHARGE syndrome: radiologic spectrum of findings. AJNR Am J Neuroradiol. 2006; 27:1663–71. [PubMed: 16971610]

Morsli H, Choo D, Ryan A, Johnson R, Wu DK. Development of the mouse inner ear and origin of its sensory organs. J Neurosci. 1998; 18:3327–35. [PubMed: 9547240]

Morsli H, Tuorto F, Choo D, Postiglione MP, Simeone A, Wu DK. Otx1 and Otx2 activities are required for the normal development of the mouse inner ear. Development. 1999; 126:2335–43. [PubMed: 10225993]

Pauley S, Wright TJ, Pirvola U, Ornitz D, Beisel K, Fritzsch B. Expression and function of FGF10 in mammalian inner ear development. Dev Dyn. 2003; 227:203–15. [PubMed: 12761848]

Raft S, Nowotschin S, Liao J, Morrow BE. Suppression of neural fate and control of inner ear morphogenesis by Tbx1. Development. 2004; 131:1801–12. [PubMed: 15084464]

Randall V, McCue K, Roberts C, Kyriakopoulou V, Beddow S, Barrett AN, Vitelli F, Prescott K, Shaw-Smith C, Devriendt K, Bosman E, Steffes G, Steel KP, Simrick S, Basson MA, Illingworth E, Scambler PJ. Great vessel development requires biallelic expression of Chd7 and Tbx1 in pharyngeal ectoderm in mice. J Clin Invest. 2009; 119:3301–3310. [PubMed: 19855134]

Salminen M, Meyer BI, Bober E, Gruss P. Netrin 1 is required for semicircular canal formation in the mouse inner ear. Development. 2000; 127:13–22. [PubMed: 10654596]

Sanchez-Calderon H, Milo M, Leon Y, Varela-Nieto I. A network of growth and transcription factors controls neuronal differentation and survival in the developing ear. Int J Dev Biol. 2007; 51:557–70. [PubMed: 17891717]

Schnetz MP, Bartels CF, Shastri K, Balasubramanian D, Zentner GE, Balaji R, Zhang X, Song L, Wang Z, Laframboise T, Crawford GE, Scacheri PC. Genomic distribution of CHD7 on chromatin tracks H3K4 methylation patterns. Genome Res. 2009; 19:590–601. [PubMed: 19251738]

Takada I, Mihara M, Suzawa M, Ohtake F, Kobayashi S, Igarashi M, Youn MY, Takeyama K, Nakamura T, Mezaki Y, Takezawa S, Yogiashi Y, Kitagawa H, Yamada G, Takada S, Minami Y, Shibuya H, Matsumoto K, Kato S. A histone lysine methyltransferase activated by non-canonical Wnt signalling suppresses PPAR-gamma transactivation. Nat Cell Biol. 2007; 9:1273–85. [PubMed: 17952062]

Tsai H, Hardisty RE, Rhodes C, Kiernan AE, Roby P, Tymowska-Lalanne Z, Mburu P, Rastan S, Hunter AJ, Brown SD, Steel KP. The mouse slalom mutant demonstrates a role for Jagged1 in neuroepithelial patterning in the organ of Corti. Hum Mol Genet. 2001; 10:507–12. [PubMed: 11181574]

Vissers LE, van Ravenswaaij CM, Admiraal R, Hurst JA, de Vries BB, Janssen IM, van der Vliet WA, Huys EH, de Jong PJ, Hamel BC, Schoenmakers EF, Brunner HG, Veltman JA, van Kessel AG. Mutations in a new member of the chromodomain gene family cause CHARGE syndrome. Nat Genet. 2004; 36:955–7. [PubMed: 15300250]

Wang W, Van De Water T, Lufkin T. Inner ear and maternal reproductive defects in mice lacking the Hmx3 homeobox gene. Development. 1998; 125:621–34. [PubMed: 9435283]

Wiener-Vacher SR, Amanou L, Denise P, Narcy P, Manach Y. Vestibular function in children with the CHARGE association. Arch Otolaryngol Head Neck Surg. 1999; 125:342–7. [PubMed: 10190809]

Winnier G, Blessing M, Labosky PA, Hogan BL. Bone morphogenetic protein-4 is required for mesoderm formation and patterning in the mouse. Genes Dev. 1995; 9:2105–16. [PubMed: 7657163]

Woodage T, Basrai MA, Baxevanis AD, Hieter P, Collins FS. Characterization of the CHD family of proteins. Proc Natl Acad Sci U S A. 1997; 94:11472–7. [PubMed: 9326634]

Highlights

- *Chd7*$^{Gt/+}$ mice exhibit delayed semicircular canal genesis and *Netrin1* expression.
- Expression of *Otx1*, *Jag1* and *Sox2* is reduced in *Chd7* mutant otocysts.
- *Bmp2* expression is reduced in the lateral canal genesis zone of *Chd7*$^{Gt/+}$ mice.
- Expression of *Bmp4, Gata3, Fgf10, Lmo4,* and *Msx1* in the developing cristae is sensitive to *Chd7* dosage.
- *Chd7* may be a selector gene for semicircular canal genesis.

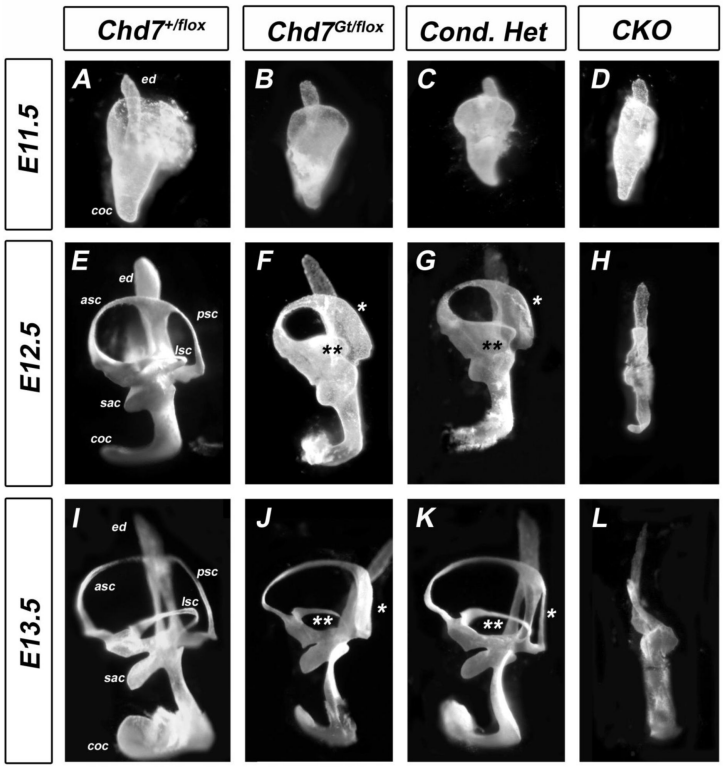

Figure 1. Posterior and lateral canal development is delayed in *Chd7* mutant embryos

Chd7$^{+/flox}$ (A,E,I), *Chd7*$^{Gt/flox}$ (B,F,J), *Chd7* conditional heterozygous (C,G,K) and *Chd7* conditional null (D,H,L) inner ears after paint filling at E11.5-E13.5. (A-D) At E11.5, anterior and posterior pouches are observed in control (A), heterozygous (B) and conditional heterozygous (C) inner ears, but are hypoplastic in CKO (D). (E-G) At E12.5, formation of the posterior (*) and lateral (**) canals are delayed in heterozygous (F) and conditional heterozygous (G) ears. By E13.5, defects in posterior (*) and lateral (**) canals are observed in heterozygous (J) and conditional heterozygous (K) ears. No canals are present in CKO inner ears at either E12.5 (H) or E13.5 (L). Abbreviations: CKO= *Chd7* conditional knockout (*Foxg1-Cre;Chd7*$^{Gt/flox}$); asc, anterior semicircular canal; coc, cochlea; ed, endolymphatic duct; lsc, lateral semicircular canal; psc, posterior semicircular canal; sac, saccule.

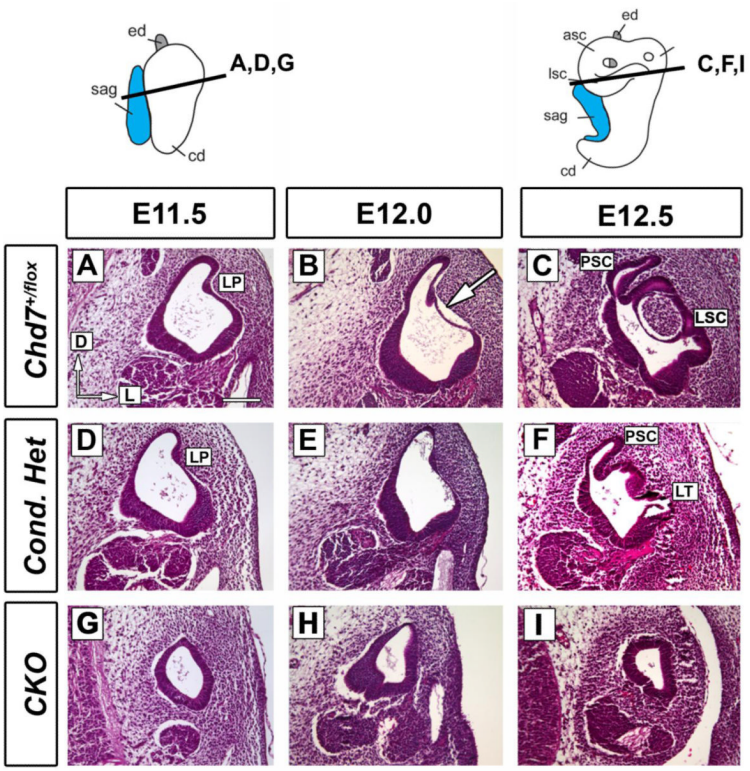

Figure 2. Lateral semicircular canal fusion is delayed in *Chd7* mutant embryos

Thin paraffin sections (7 μm) cut in the transverse plane at E11.5 (A, D, G), E12.0 (B, E, H) and E12.5 (C, F, I) were stained with Hematoxylin and Eosin at the level of the lateral canal. (A-C) Control (*Chd7*$^{+/flox}$) semicircular canal epithelium detaches from the basement membrane (arrow) creating the lateral semicircular canal (LC). (D-F) Conditional heterozygous (*Foxg1-Cre;Chd7*$^{+/flox}$) inner ears exhibit delayed epithelial detachment (E vs. B), resulting in a truncated lateral semicircular canal (LT in F). (G-I) The CKO (*Foxg1-Cre;Chd7*$^{Gt/flox}$) vestibule displays a very small canal outpocketing (G) and no visible fusion plate or lateral semicircular canal (H-I). Orientation: dorsal is towards the top and lateral is to the right, as shown in (A). Other abbreviations: CKO, *Chd7* conditional knockout (*Foxg1-Cre;Chd7*$^{Gt/flox}$); LP, lateral pouch; LSC, lateral semicircular canal; LT, lateral truncation; PSC, posterior semicircular canal. Bar in A= 100 μm and applies to all panels.

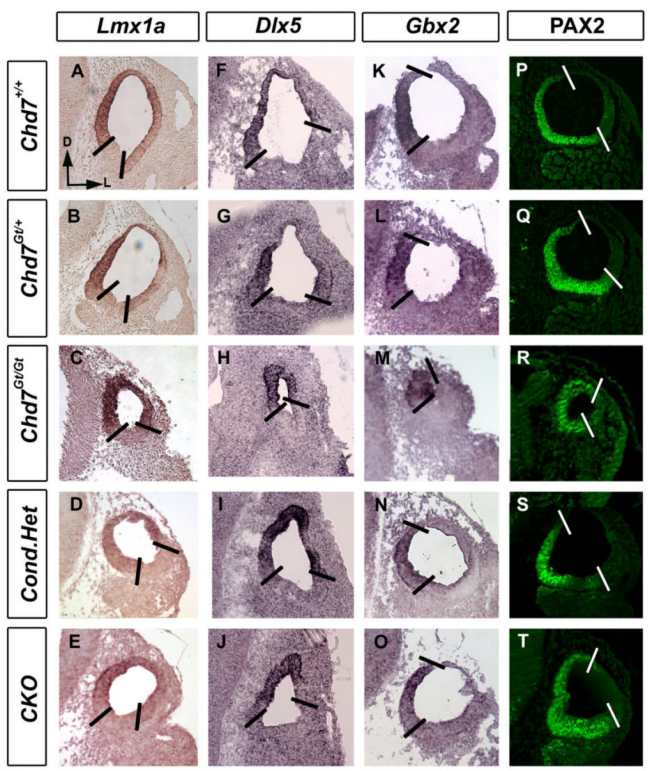

Figure 3. Dorsomedial markers are unchanged in *Chd7* mutant mice

In situ hybridization and immunofluorescence with probes against *Lmx1a* (A-E), *Dlx5* (F-J), *Gbx2* (K-O) and anti-PAX2 (P-T) shows unaltered expression patterns between E10.5 $Chd7^{+/+}$ (A, F, K ,P), $Chd7^{Gt/+}$ (B, G, L, Q), $Chd7^{Gt/Gt}$ (C, H, M, R), *Foxg1-Cre;*$Chd7^{+/flox}$ (D, I, N, S) and *Foxg1-Cre;*$Chd7^{Gt/flox}$ (E, J, O, T) otocysts. All sections are in the transverse orientation with dorsal towards the top as shown by the arrows in (A). Bold lines delimit expression domains. Abbreviation: CKO= *Chd7* conditional knockout (*Foxg1-Cre;*$Chd7^{Gt/flox}$).

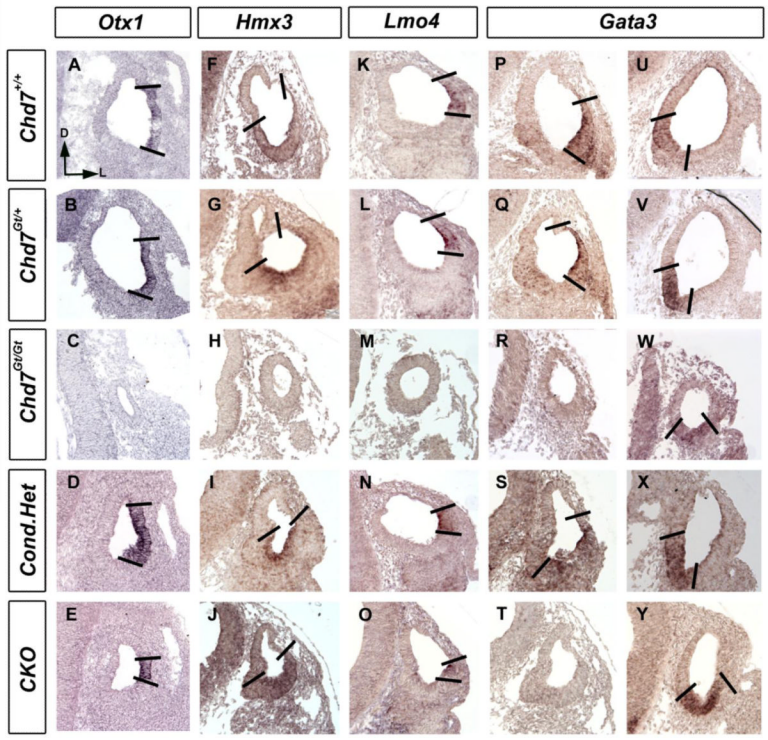

Figure 4. Expression of genes in the lateral otocyst is reduced in *Chd7* null mutant embryos

In situ hybridization with probes against *Otx1* (A-E), *Hmx3* (F-J), *Lmo4* (K-O) and *Gata3* (P-Y) shows unchanged expression in E10.5 $Chd7^{+/+}$ (A, F, K, P, U), $Chd7^{Gt/+}$ (B, G, L, Q, V) and *Foxg1-Cre;*$Chd7^{+/flox}$ (D, I, N, S, X). *Otx1* (E) and dorsal *Gata3* (T) expression are reduced in CKO embryos, whereas *Hmx3* (J), *Lmo4* (O), and ventral *Gata3* (Y) expression are preserved. Hypoplastic $Chd7^{Gt/Gt}$ otocysts show no *Otx1*, *Hmx3*, *Lmo4* or dorsal *Gata3* expression, but maintain ventral *Gata3* expression (W). All sections are in the transverse orientation with dorsal towards the top as shown by the arrows in (A). Bold lines delimit expression domains. Abbreviation: CKO = *Chd7* conditional knockout (*Foxg1-Cre;*$Chd7^{Gt/flox}$).

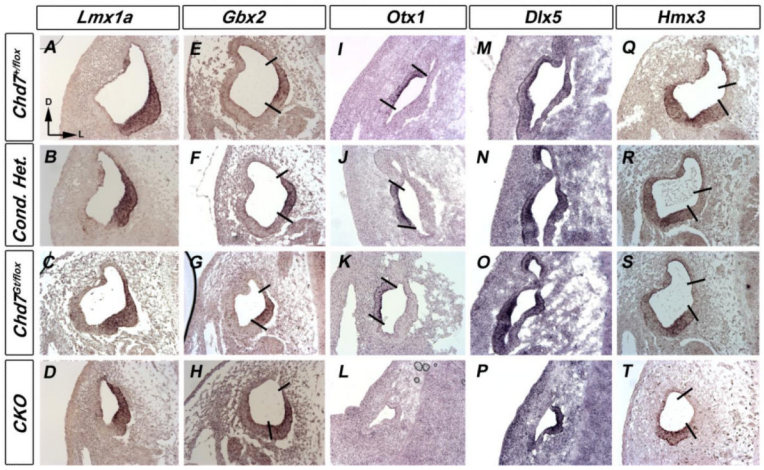

Figure 5. *Otx1* expression is reduced in *Chd7* mutant embryos

In situ hybridization with probes against *Lmx1a* (A-D), *Gbx2* (E-H), *Otx1* (I-L), *Dlx5* (M-P) and *Hmx3* (Q-T) show unaltered expression patterns in E11.5 $Chd7^{+/flox}$ (A, E, I, M, Q), conditional heterozygous (B, F, J, N, R) and $Chd7^{Gt/+}$ (C, G, K, O, S) ears. *Lmx1a* (D), *Gbx2* (H), *Hmx3* (T) and medial *Dlx5* (P) expression were preserved in *Chd7* CKO (*Foxg1-Cre;*$Chd7^{Gt/flox}$) ears. Lateral *Dlx5* (P) and *Otx1* (L) expression were absent from CKO inner ears. All sections are in the transverse orientation at the level of the lateral semicircular canal. Bold lines delimit expression domains. Abbreviation: CKO= *Chd7* conditional knockout (*Foxg1-Cre;*$Chd7^{Gt/flox}$).

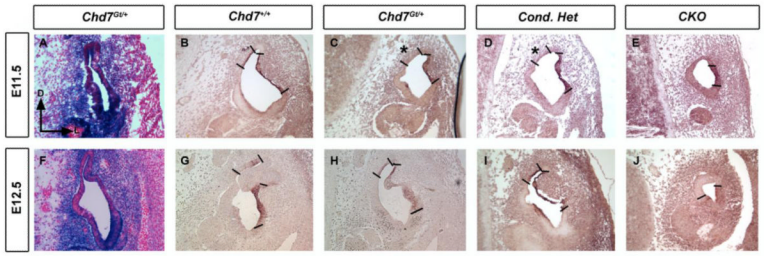

Figure 6. Medial *Netrin1* expression is delayed in *Chd7* mutant semicircular canal primordia

Transverse sections at the level of the lateral semicircular canal primordia at E11.5 (A-E) and E12.5 (F-J) were stained for β-galactosidase activity (A, F) or *Netrin1* mRNA (B-E,G-J). (A, F) β-galactosidase activity shows *Chd7* promoter activity within the periotic mesenchyme surrounding the semicircular canals and within the primordial canal epithelium. *In situ* hybridization shows medial (*) and lateral expression of *Netrin1.* Medial *Netrin1* expression (*) is delayed in E11.5 germline and conditional *Chd7* heterozygotes (C,D) . The entire *Netrin1* expression domain is reduced in hypoplastic *Foxg1-Cre;Chd7*$^{Gt/flox}$ (I, J) inner ear. Bold lines delimit *Netrin1* expression domains. Orientation for all panels is shown by the arrows in (A). Bar in A= 100 μm and applies to all panels. Abbreviation: CKO= *Chd7* conditional knockout (*Foxg1-Cre;Chd7*$^{Gt/flox}$).

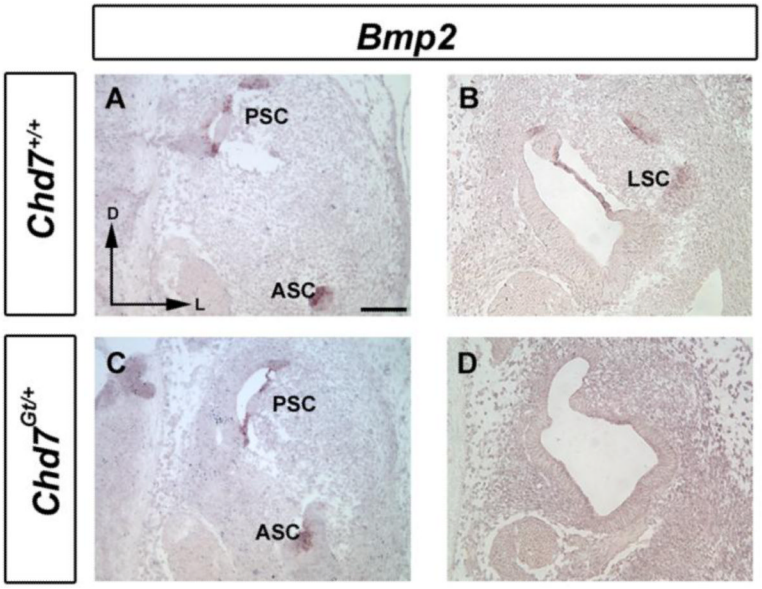

Figure 7. *Bmp2* expression is reduced in *Chd7*$^{Gt/+}$ inner ears

In situ hybridization of E12.5 transverse sections of wild type (A,B) and *Chd7*$^{Gt/+}$ (C, D) embryos shows selective absence of *Bmp2* mRNA from the *Chd7*$^{Gt/+}$ lateral canal region (D), despite normal expression in anterior and posterior regions (C). Orientation: dorsal towards the top and lateral to the right, as shown by the arrows in (A). Abbreviations: AC, Anterior semicircular canal; LC, Lateral semicircular canal; PC, posterior semicircular canal.

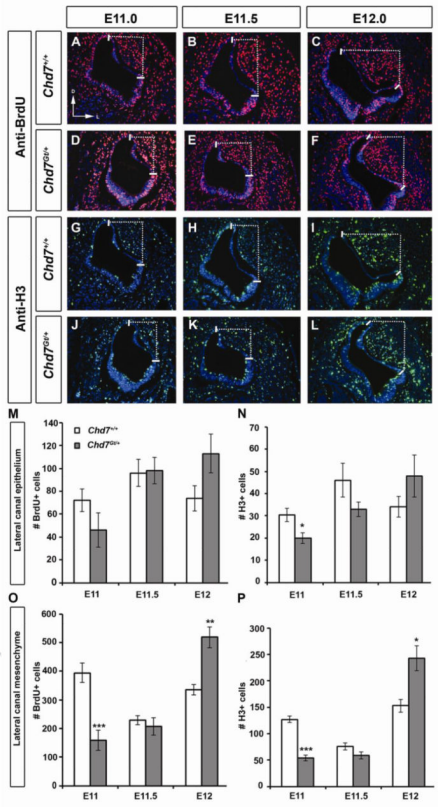

Figure 8. Proliferation is altered in the lateral canal epithelium and mesenchyme of *Chd7*$^{Gt/+}$ embryos

Double immunofluorescence for anti-BrdU and anti-H3 of wild type (A-C, G-I) and *Chd7*$^{Gt/+}$ (D-F, J-L) lateral semicircular canals at E11.0 (A,D,G,J), E11.5 (B,E,H,K) and E12.0 (C,F,I,L). Numbers of proliferating cells were counted in the lateral epithelium (between solid lines; M,N) and in the lateral periotic mesenchyme (within dotted lines; O,P). At E11.0, significant decrease in H3-positive cells in the *Chd7*$^{Gt/+}$ epithelium (N) and mesenchyme (P), and BrdU-positive cells in *Chd7*$^{Gt/+}$ mesenchyme (O) were observed. Increased BrdU-positive and H3-positive cells were observed in *Chd7*$^{Gt/+}$ mesenchyme at E12.0 (N,P) compared to wild type controls. Sections are in the transverse plane, with dorsal towards the top as in (A). **P<0.05*, ***P<0.01*, ****P<0.001*.

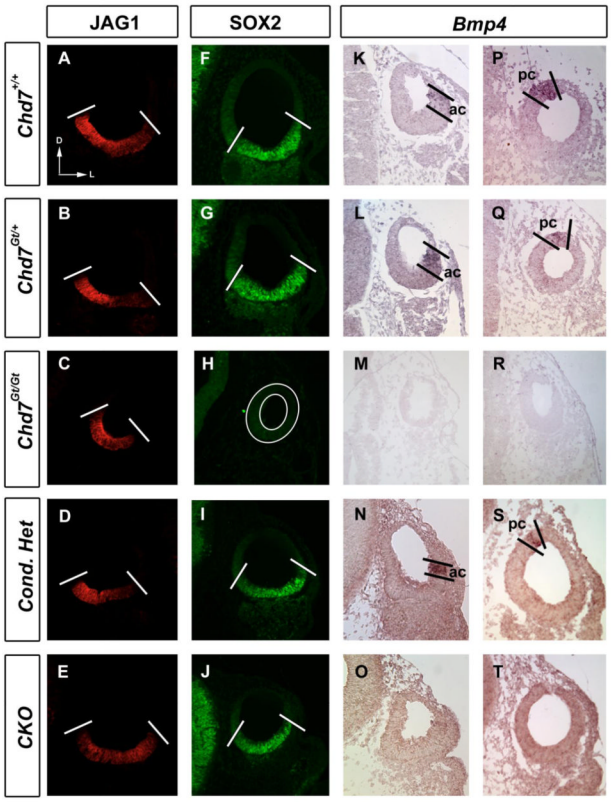

Figure 9. *Bmp4* and SOX2 in the developing crista are sensitive to *Chd7* dosage

Immunofluorescence (A-J) or *in situ* hybridization (K-T) of E10.5 transverse sections. JAGGED1 is unaltered in *Chd7* heterozygous (B, D) and *Chd7* null (C, E) otocysts compared to control otocysts (A). SOX2 is unchanged in *Chd7* heterozygous (G, I) and conditional null (J) otocysts but is absent from $Chd7^{Gt/Gt}$ (H) otocysts. *Bmp4* is expressed within the anterior crista primordia (ac) in *Chd7* heterozygous mutants (L, N) and is variably expressed in the posterior crista primordia (pc); some otocysts display positive *Bmp4* expression in the posterior streak (Q, S) whereas it is absent from other otocysts. *Bmp4* expression is absent from *Chd7* null mutant otocyst (M, O). Bold lines delineate expression domains. Plane of section is shown by arrows in (A), with dorsal toward the top and lateral toward the right. Abbreviation: CKO= *Chd7* conditional knockout (*Foxg1-Cre;*$Chd7^{Gt/flox}$).

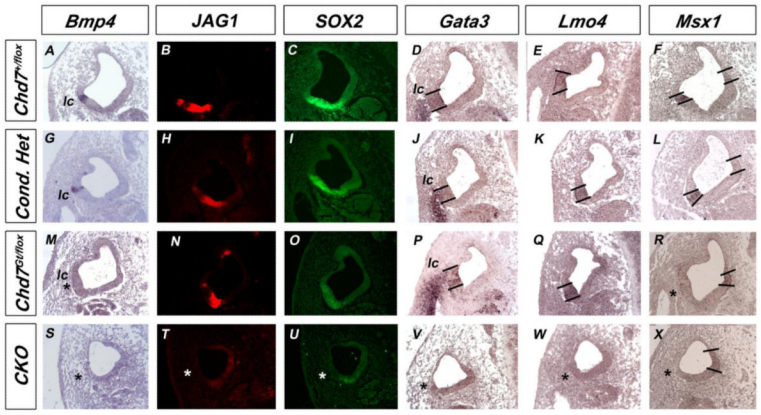

Figure 10. Expression of genes expressed in the lateral crista is altered in *Chd7* mutant embryos

In situ hybridization (A, D-G, J-M, P-S, V-X) or immunofluorescence (B, C, H, I, N, O, T, U) of E11.5 transverse sections at the level of the lateral canal. *Bmp4,* JAG1, SOX2*, Gata3, Lmo4 and Msx1* are present within the lateral crista primordium (lc) in conditional heterozygous mutants (G-L), but absent from CKO otocysts (* in S-X). *Bmp4* expression is variably absent in $Chd7^{Gt/flox}$ otocysts (* in M), but JAG1 and SOX2 are preserved in adjacent sections (N, O). Expression of *Gata3* and *Lmo4* are unchanged in $Chd7^{Gt/flox}$ otocysts (P,Q), but lateral expression of *Msx1* is absent (* in R). Bold lines delineate expression domains. Abbreviation: CKO= *Chd7* conditional knockout (*Foxg1-Cre;*$Chd7^{Gt/flox}$).

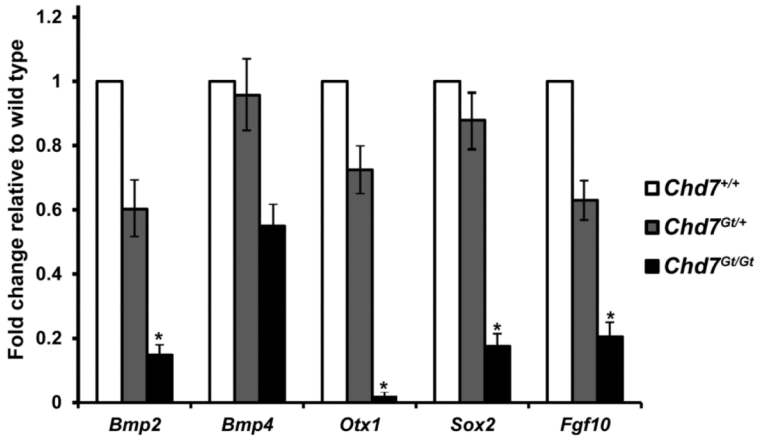

Figure 11. *Bmp2, Bmp4, Otx1, Sox2* and *Fgf10* in the otocyst are regulated by *Chd7* in a dosage dependent manner

qRT-PCR analysis of total RNA from E10.5 *Chd7*$^{+/+}$, *Chd7*$^{Gt/+}$ and *Chd7*$^{Gt/Gt}$ microdissected inner ears shows dosage sensitive reductions with loss of *Chd7*. Threshold cycles from the experimental genes were normalized to *Gapdh,* and the *Chd7*$^{Gt/+}$ and *Chd7*$^{Gt/Gt}$ were compared to wild type (*Chd7*$^{+/+}$). Error bars are standard error of the mean, n=3 for each genotype. *$P<0.05$

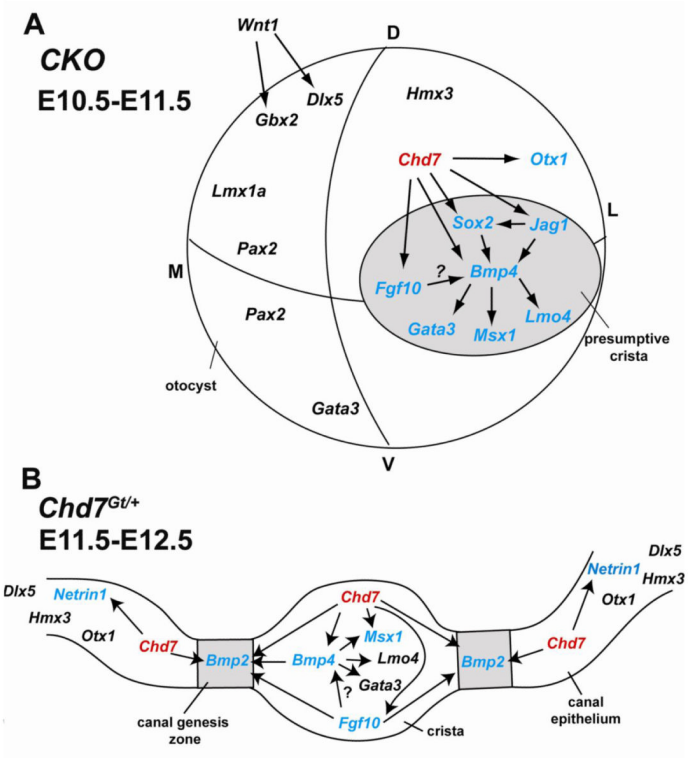

Figure 12. Model of *Chd7* function in genetic cascades that regulate lateral semicircular canal development

(A) Conditional loss of *Chd7* using *Foxg1-Cre* results in reduced expression of *Bmp4, Sox2, Otx1, Jag1, Fgf10, Gata3, Msx1* and *Lmo4* in the dorsal otocyst and presumptive crista (grey circle). (B) Heterozygous loss of *Chd7* (red) results in down-regulation of *Fgf10*, *Bmp4* and *Msx1* in the lateral crista and *Bmp2* in the lateral canal genesis zone (grey boxes), either directly or indirectly through *Fgf10* and *Bmp4*. *Netrin1* expression in the lateral canal epithelium is positively regulated by *Chd7*. Genes shown in black are unchanged and genes shown in blue are changed by reduced *Chd7*.

Table 1

Summary of gene expression in *Chd7* mutant embryos in the inner ear

	+/+		Gt/+		Gt/Gt	Cond. het		CKO	
	E10.5	E11.5	E10.5	E11.5	E10.5	E10.5	E11.5	E10.5	E11.5
***Bmp4* , anterior**	+	+	+	+	−	+	+	−	−
***Bmp4* , posterior**	+	+	var	+	−	+	+	−	−
***Bmp4* , lateral**	n.d.	+	n.d.	var	n.d.	n.d.	+	n.d.	−
***Bmp2* , AP**	n.d.	+	n.d.	+	n.d.	n.d.	n.d.	n.d.	n.d.
***Bmp2* , lateral**	n.d.	+	n.d.	−	n.d.	n.d.	n.d.	n.d.	n.d.
Dlx5	+	+	+	+	+	+	+	+	+
Gbx2	+	+	+	+	+	+	+	+	+
***Gata3* , dorsal**	+	+	+	+	−	+	+	−	−
***Gata3* , ventral**	+	n.d.	+	n.d.	+	+	n.d.	+	n.d.
Hmx3	+	+	+	+	−	+	+	+	+
JAG1	+	+	+	+	+	+	+	+	−
Lmx1a	+	+	+	+	+	+	+	+	+
Lmo4	+	+	+	+	−	+	+	+	−
Msx1	n.d.	+	n.d.	−	n.d.	n.d.	+	n.d.	−
Netrin1	n.d.	+	n.d.	del	n.d.	n.d.	del	n.d	−
Otx1	+	+	+	+	−	+	+	red	−
PAX2	+	n.d.	+	n.d.	+	+	n.d.	+	n.d.
SOX2	+	+	+	+	−	+	+	+	−

Abbreviations: del, delayed; n.d., not determined; var, variable